CHAPTER-5

THE EFFECT OF HALL CURRENT ON AN UNSTEADY MHD FLOW ALONG A FLAT PLATE WITH VISCOUS DISSIPATION AND HEAT ABSORPTION

5.1 INTRODUCTION

Considerable attention has been given to the unsteady free convection flow of viscous incompressible, electrically conducting fluid in presence of applied magnetic field in connection with the theories of fluid motion in the liquid core of the Earth and also meteorological and oceanographic applications. In recent years, the analysis of hydromagnetic flow involving heat and mass transfer in porous medium has attracted the attention of many scholars because of its possible applications in diverse fields of science and technology such as–soil sciences, astrophysics, geophysics, nuclear power reactors etc. In geophysics, it finds its applications in the design of MHD generators and accelerators, underground water energy storage system etc. It is worth–mentioning that MHD is now undergoing a stage of great enlargement and differentiation of subject matter. These new problems draw the attention of the researchers due to their varied significance, in liquid metals, electrolytes and ionized gases etc. In addition, the applications of the effect of Hall current on the fluid flow with variable concentration have been seen in MHD power generators, astrophysical and meteorological studies as well as in plasma physics. The Hall Effect is due merely to the sideways magnetic force on the drifting free charges. The electric field has to have a component transverse to the direction of the current density to balance this force. In many works on plasma physics, the Hall Effect is disregarded. But if the strength of magnetic field is high and the number density of electrons is small, the Hall Effect cannot be ignored as it has a significant effect on the flow pattern of an ionized gas. Hall Effect results in a development of an additional potential difference between opposite surfaces of a conductor for which a current is induced perpendicular to both the electric and magnetic field. This current is termed as Hall current. Model studies on the effect of Hall current on MHD convection flows have been carried out by many authors due to application of such studies in the problems of MHD generators and Hall accelerators.

From the point of view of applications, this effect can be taken into account within the range of magnetohydrodynamical approximation. Abdul Maleque *et al.* [1] studied the effects of variable properties and Hall current on steady MHD laminar convective fluid flow due to a porous rotating disk. Ajay Kumar Singh [2] made an attempt to study the steady MHD free convection and mass transfer flow with hall current, viscous dissipation and joule heating, taking in to account the thermal diffusion

effect. Alam *et al.* [3] have studied unsteady free convective heat and mass transfer flow in a rotating system with Hall currents, viscous dissipation and Joul heating. Anand Rao *et al.* [4] investigated applied magnetic field on transient free convective flow of an incompressible viscous dissipative fluid in a vertical channel. Anand Rao and Srinivasa Raju [5] studied the effect of hall current on an unsteady magnetohydrodynamic flow past along a porous flat plate with heat and mass transfer in presence of viscous dissipation. Anjali Devi *et al.* [6] discussed pulsated convective MHD flow with Hall current, heat source and viscous dissipation along a vertical porous plate. Atul Kumar Singh *et al.* [7] studied hydromagnetic free convection and mass transfer flow with Joule heating, thermal diffusion, Heat source and Hall current. Chamkha [8] investigated unsteady convective heat and mass transfer past a semi-infinite permeable moving plate with heat absorption where it was found that increase in solutal Grashoff number enhanced the concentration buoyancy effects leading to an increase in the velocity. Chaudhary *et al.* [9] analyzed Hall Effect on MHD mixed convection flow of a viscoelastic fluid past an infinite vertical porous plate with mass transfer and radiation. Chowdhary *et al.* [10] studied heat and mass transfer in elasticoviscous fluid past an impulsively started infinite vertical plate with Hall Effect. Cookey *et al.* [11] studied influence of viscous dissipation and radiation on unsteady MHD free convection flow past an infinite heated vertical plate in a porous medium with time dependent suction. On the effectiveness of viscous dissipation and Joule heating on steady MHD and slip flow of a bingham fluid over a porous rotating disk in the presence of Hall and ion-slip currents was studied by Emmanuel Osalusi *et al.* [12].

Hossain *et al.* [13] investigated the effect of hall current on the unsteady free convection flow of a viscous incompressible fluid with heat and mass transfer along a vertical porous plate subjected to a time dependent transpiration velocity when the constant magnetic field is applied normal to the flow. Lai [14] studied the coupled heat and mass transfer by mixed convection from vertical plate in a saturated porous medium. Maleque *et al.* [15] investigated the effects of variable properties and hall current on steady MHD laminar convective fluid flow due to a porous rotating disk. MHD stationary symmetric flows with Hall effect was analyzed by Palumbo *et al.* [16]. Raja Shekhar *et al.* [17] studied the effect of hall current on free convection and mass transfer flow through a porous medium bounded by an infinite vertical porous plate, when the plate

was subjected to a constant suction velocity and heat flux. Singh *et al.* [18] studied the effects of mass transfer on the flow past a vertical porous plate. Singh *et al.* [19] studied an integral treatment for combined heat and mass transfer by natural convention in a porous medium. Singh *et al.* [20] analyzed the free convection heat and mass transfer along a vertical surface in a porous medium. Later, Soundalgekar *et al.* [21] studied the coupled heat and mass transfer by natural convection from vertical surfaces in a porous medium. Hall Effect on MHD Flow and Heat Transfer along a Porous Flat Plate with Mass Transfer and Source/Sink was analyzed by Srihari *et al.* [22]. Sriramulu *et al.* [23] discussed the effect of Hall Current on MHD flow and heat transfer along a porous flat plate with mass transfer.

In view of the above observations the main objective of this chapter is to study the Hall Effect on MHD flow and mass transfer of an electrically conducting incompressible fluid along an infinite vertical porous plate with viscous dissipation and heat source. Also, the effects of different flow parameters encountered in the equations are studied. The results obtained are good agreement with the results of Sriramulu *et al.* [23]. The problem is governed by system of coupled non–linear partial differential equations whose exact solution is difficult to obtain. Hence, the problem is solved by using Galerkin finite element method, which is more economical from computational view point.

5.2 FORMULATION OF THE PROBLEM

We consider the effects of hall current and heat absorption on an unsteady free convection flow of an incompressible, viscous, electrically conducting fluid with mass transfer along a porous flat plate with viscous dissipation has been studied. The flow is assumed to be in x' – direction, which is taken along the plate in upward direction. The y' – direction which is taken along the normal to the direction of the plate. Initially, for time $t' \leq 0$, the plate and the fluid are maintained at the same constant temperature T_∞ in a stationary condition with the same species concentration C_∞ at all points so that, the Soret and Dufour effects are neglected. When $t' > 0$, the temperature of the plate is instantaneously raised (or lowered) to T_w and the concentration of the species is raised (or lowered) to C_w, which are hereafter regarded as constant. We also assumed that the level of species concentration is very low and hence species thermal diffusion and diffusion thermal energy effects can be neglected. A magnetic field of uniform strength is

applied normal to the porous plate. The magnetic Reynolds number of the flow is taken to be small enough so that the induced magnetic field can be neglected.

Using the relation $\nabla.\overline{H}=0$ for the magnetic field $\overline{H}=(H_x,H_y,H_z)$, we obtain H_y = constant = H_o (say) where H_o is the externally applied transverse magnetic field so that $\overline{H}=(0,H_o,0)$. The equation of conservation of electric charge $\nabla.\overline{J}=0$ gives j_y = constant, where $\overline{J}=(j_x,j_y,j_z)$. We further assume that the plate is non-conducting. This implies $j_y=0$ at the plate and hence zero everywhere. When the strength of magnetic field is very large, the generalized Ohm's law in the absence of electric field takes the following form:

$$\overline{J}+\frac{\omega_e\tau_e}{B_o}\overline{J}\times\overline{H}=\sigma\left(\mu_e\overline{V}\times\overline{H}+\frac{1}{en_e}\nabla P_e\right) \tag{1}$$

Under the assumption that the electron pressure (for weakly ionized gas), the thermo-electric pressure and ion-slip conditions are negligible, equation (1) becomes:

$$j_x=\frac{\sigma\mu_e H_o}{1+m^2}\left(mu'-w'\right)\text{and}\quad j_z=\frac{\sigma\mu_e H_o}{1+m^2}\left(mw'+u'\right) \tag{2}$$

Where u' is the x'-component of $\overline{V}$, w' is the z'-component of $\overline{V}$ and $m(=\omega_e\tau_e)$ is the hall parameter. Within the above framework, the equations which govern the flow under the usual Boussinesq's approximation are as follows:

$$\frac{\partial v'}{\partial y'}=0 \tag{3}$$

$$\frac{\partial u'}{\partial t'}+v'\frac{\partial u'}{\partial y'}=\upsilon\frac{\partial^2 u'}{\partial y'^2}-\frac{\sigma\mu^2_e H^2_o}{\rho\left(1+m^2\right)}\left(u'+mw'\right)+g\beta\left(T-T_\infty\right)+g\beta^*\left(C'-C'_\infty\right) \tag{4}$$

$$\frac{\partial w'}{\partial t'}+v'\frac{\partial w'}{\partial y'}=\upsilon\frac{\partial^2 w'}{\partial y'^2}-\frac{\sigma\mu^2_e H^2_o}{\rho\left(1+m^2\right)}\left(w'-mu'\right) \tag{5}$$

$$\frac{\partial T}{\partial t'}+v'\frac{\partial T'}{\partial y'}=\frac{k}{\rho C_p}\frac{\partial^2 T}{\partial y'^2}+\frac{\upsilon}{C_p}\left(\frac{\partial u'}{\partial y'}\right)^2-\frac{Q_o}{\rho C_p}(T-T_\infty) \tag{6}$$

$$\frac{\partial C}{\partial t'}+v'\frac{\partial C'}{\partial y'}=D\frac{\partial^2 C'}{\partial y'^2} \tag{7}$$

The initial and boundary conditions of the problem are:

$$t' \le 0:\ u' = 0,\quad w' = 0,\ T = T_\infty,\ C' = C_\infty \quad for\ all\ \ y'$$
$$t' > 0: \begin{cases} u' = 0,\quad w' = 0,\ T = T_w,\ C' = C_w & at\quad y' = 0 \\ u' = 0,\quad w' = 0,\ T = T_\infty,\ C' = C_\infty & as\quad y' \to \infty \end{cases} \qquad (8)$$

Where (u', v', w'), Dimensional velocity components; $(x,' y')$, Dimensional Cartesian coordinates; T_w , Wall temperature; T_∞, temperature of the fluid for away from the plate the plate ; t', Dimensional time; C'_w,Concentration near the plate; C'_∞, Concentration in the fluid for away from the plate the plate; ρ, Density, kg/m^3; g, Acceleration due to gravity, 9.81m/s^2; C_p,Specific heat capacity; k, Thermal conductivity, W/mK; α, Thermal diffusivirty; U_0, Reference velocity; σ, Electrical conductivity; Q_0, Dimensional heat absorption coefficient; υ, Kinematic coefficient; μ, Viscosity, Ns/m^2; m, Hall parameter; ε, Porosity of the porous medium; β, Coefficients of volume expansion due to temperature; β^*, Coefficient of volume expansion due to concentration; D, Chemical diffusivity; e the electron charge, ω_e, electron frequency, radian/sec; τ_e, electron collision time in sec, p_e, electron pressure, $\vec{E}$, electric field and η_e, number density of electron; μ_e, Magnetic permeability.

The non – dimensional quantities introduced in the equations (3) – (7) are:

$$\left.\begin{aligned} & t = \frac{t' U_o^2}{\upsilon},\ y = \frac{y' U_0}{\upsilon},\ (u, v, w) = \frac{(u', v', w')}{U_o}, \theta = \frac{(T - T_\infty)}{(T_w - T_\infty)}, \\ & C = \frac{(C' - C_\infty)}{(C_w - C_\infty)}, M = \frac{\sigma \mu_e^2 H_0^2 \upsilon}{\rho U_o^2},\ \Pr = \frac{\mu C_p}{k},\ Ec = \frac{U_o^2}{C_p (T_w - T_\infty)}, \\ & Sc = \frac{\upsilon}{D}, Gr = \frac{\upsilon g \beta (T_w - T_\infty)}{U_o^3}, Gc = \frac{\upsilon g \beta^* (C_w - C_\infty)}{U_o^3}, Q = \frac{\upsilon Q_o}{\rho C_p U_o^2}, \end{aligned}\right\} \qquad (9)$$

The governing equations can be obtained in the dimensionless form as:

$$\frac{\partial v}{\partial y}=0 \tag{10}$$

$$\frac{\partial u}{\partial t}+v\frac{\partial u}{\partial y}=\frac{\partial^2 u}{\partial y^2}-\frac{M}{\left(1+m^2\right)}\left(u+mw\right)+(Gr)\theta+(Gc)C \tag{11}$$

$$\frac{\partial w}{\partial t}+v\frac{\partial w}{\partial y}=\frac{\partial^2 w}{\partial y^2}-\frac{M}{\left(1+m^2\right)}\left(w-mu\right) \tag{12}$$

$$\frac{\partial \theta}{\partial t}+v\frac{\partial \theta}{\partial y}=\frac{1}{\Pr}\frac{\partial^2 \theta}{\partial y^2}+(Ec)\left(\frac{\partial u}{\partial y}\right)^2-Q\theta \tag{13}$$

$$\frac{\partial C}{\partial t}+v\frac{\partial C}{\partial y}=\frac{1}{Sc}\frac{\partial^2 C}{\partial y^2} \tag{14}$$

Where M, Hartmann number; Pr, Prandtl number; Sc, Schmidt number; Ec, Eckert number; θ, Non–dimensional temperature; C, Non – dimensional species concentration; Gr, Grashof number; Gc, Modified Grashof number; Q, Heat source.

The initial and boundary conditions (8) in the non – dimensional form are:

$$t\le 0:\quad u=0,\ w=0,\ \theta=0, C=0 \quad for\ all\ \ y$$
$$t>0:\quad \begin{cases} u=0,\ w=0,\ \theta=1,\ C=1 & at\ y=0 \end{cases} \tag{15}$$

From equation (10), we see that v is either constant or a function of time t. Similarly solutions of equations (11) – (14) with the boundary conditions (15) exists only if we take

$$v=\lambda t^{\frac{-1}{2}} \tag{16}$$

where λ is a non – dimensional transpiration parameter. For suction $\lambda>0$ and for blowing $\lambda<0$. From (16), it can be observed that the assumption is valid only for small values of time variable.

5.3 METHOD OF SOLUTION

By applying Galerkin finite element method for equation (11) over the element (e), $(y_j \le y \le y_k)$ is:

$$\int_{y_j}^{y_k}\left\{N^{(e)T}\left[\frac{\partial^2 u^{(e)}}{\partial y^2}-\frac{\partial u^{(e)}}{\partial t}-\nu\frac{\partial u^{(e)}}{\partial y}-Au^{(e)}+P\right]\right\}dy=0 \qquad (17)$$

where $A=\dfrac{M}{1+m^2}$, $P=(Gr)\theta_i^j+(Gc)C_i^j-Amw_i^j$

Integrating the first term in equation (17) by parts one obtains

$$N^{(e)T}\left\{\frac{\partial u^{(e)}}{\partial y}\right\}_{y_j}^{y_k}-\int_{y_j}^{y_k}\left\{\frac{\partial N^{(e)T}}{\partial y}\frac{\partial u^{(e)}}{\partial y}+N^{(e)T}\left(\frac{\partial u^{(e)}}{\partial t}+\nu\frac{\partial u^{(e)}}{\partial y}+Au^{(e)}-P\right)\right\}dy=0 \qquad (18)$$

Neglecting the first term in equation (18), one gets:

$$\int_{y_j}^{y_k}\left\{\frac{\partial N^{(e)T}}{\partial y}\frac{\partial u^{(e)}}{\partial y}+N^{(e)T}\left(\frac{\partial u^{(e)}}{\partial t}+\nu\frac{\partial u^{(e)}}{\partial y}+Au^{(e)}-P\right)\right\}dy=0$$

Let $u^{(e)}=N^{(e)}\phi^{(e)}$ be the linear piecewise approximation solution over the element (e) $(y_j\le y\le y_k)$, where $N^{(e)}=\begin{bmatrix}N_j & N_k\end{bmatrix}$, $\phi^{(e)}=\begin{bmatrix}u_j & u_k\end{bmatrix}^T$ and $N_j=\dfrac{y_k-y}{y_k-y_j}$, $N_k=\dfrac{y-y_j}{y_k-y_j}$

are the basis functions. One obtains:

$$\int_{y_j}^{y_k}\left\{\begin{bmatrix}N_j'N_j' & N_j'N_k'\\ N_j'N_k' & N_k'N_k'\end{bmatrix}\begin{bmatrix}u_j\\ u_k\end{bmatrix}\right\}dy+\int_{y_j}^{y_k}\left\{\begin{bmatrix}N_jN_j & N_jN_k\\ N_jN_k & N_kN_k\end{bmatrix}\begin{bmatrix}\dot{u}_j\\ \dot{u}_k\end{bmatrix}\right\}dy+\nu\int_{y_j}^{y_k}\left\{\begin{bmatrix}N_j'N_j' & N_j'N_k'\\ N_j'N_k' & N_k'N_k'\end{bmatrix}\begin{bmatrix}u_j\\ u_k\end{bmatrix}\right\}dy$$

$$+A\int_{y_j}^{y_k}\left\{\begin{bmatrix}N_jN_j & N_jN_k\\ N_jN_k & N_kN_k\end{bmatrix}\begin{bmatrix}u_j\\ u_k\end{bmatrix}\right\}dy=P\int_{y_j}^{y_k}\begin{bmatrix}N_j\\ N_k\end{bmatrix}dy$$

Simplifying we get

$$\frac{1}{l^{(e)^2}}\begin{bmatrix}1 & -1\\ -1 & 1\end{bmatrix}\begin{bmatrix}u_j\\ u_k\end{bmatrix}+\frac{1}{6}\begin{bmatrix}2 & 1\\ 1 & 2\end{bmatrix}\begin{bmatrix}\dot{u}_j\\ \dot{u}_k\end{bmatrix}+\frac{\nu}{2l^{(e)}}\begin{bmatrix}-1 & 1\\ -1 & 1\end{bmatrix}\begin{bmatrix}u_j\\ u_k\end{bmatrix}+\frac{A}{6}\begin{bmatrix}2 & 1\\ 1 & 2\end{bmatrix}\begin{bmatrix}u_j\\ u_k\end{bmatrix}=\frac{P}{2}\begin{bmatrix}1\\ 1\end{bmatrix}$$

Using the above equation, in order to get the difference equation at the nodes $(y_{i-1}\le y\le y_i)$ and $(y_i\le y\le y_{i+1})$. We write the element equation for the element $(y_{i-1}\le y\le y_i)$ as

$$\frac{1}{l^{(e)2}}\begin{bmatrix}1 & -1\\ -1 & 1\end{bmatrix}\begin{bmatrix}u_{i-1}\\ u_i\end{bmatrix}+\frac{1}{6}\begin{bmatrix}2 & 1\\ 1 & 2\end{bmatrix}\begin{bmatrix}\dot{u}_{i-1}\\ \dot{u}_i\end{bmatrix}+\frac{\nu}{2l^{(e)}}\begin{bmatrix}-1 & 1\\ -1 & 1\end{bmatrix}\begin{bmatrix}u_{i-1}\\ u_i\end{bmatrix}+\frac{A}{6}\begin{bmatrix}2 & 1\\ 1 & 2\end{bmatrix}\begin{bmatrix}u_{i-1}\\ u_i\end{bmatrix}=\frac{P}{2}\begin{bmatrix}1\\ 1\end{bmatrix}$$

and for the second element $(y_i \le y \le y_{i+1})$ we get the element equation as

$$\frac{1}{l^{(e)2}}\begin{bmatrix}1 & -1\\ -1 & 1\end{bmatrix}\begin{bmatrix}u_i\\ u_{i+1}\end{bmatrix}+\frac{1}{6}\begin{bmatrix}2 & 1\\ 1 & 2\end{bmatrix}\begin{bmatrix}\dot{u}_i\\ \dot{u}_{i+1}\end{bmatrix}+\frac{\nu}{2l^{(e)}}\begin{bmatrix}-1 & 1\\ -1 & 1\end{bmatrix}\begin{bmatrix}u_i\\ u_{i+1}\end{bmatrix}+\frac{A}{6}\begin{bmatrix}2 & 1\\ 1 & 2\end{bmatrix}\begin{bmatrix}u_i\\ u_{i+1}\end{bmatrix}=\frac{P}{2}\begin{bmatrix}1\\ 1\end{bmatrix}$$

where prime and dot denotes differentiation w.r.t y and time t respectively. Assembling the above two element equations for two consecutive elements $(y_{i-1} \le y \le y_i)$ and $(y_i \le y \le y_{i+1})$ following is obtained:

$$\frac{1}{l^{(e)2}}\begin{bmatrix}1 & -1 & 0\\ -1 & 2 & -1\\ 0 & -1 & 1\end{bmatrix}\begin{bmatrix}u_{i-1}\\ u_i\\ u_{i+1}\end{bmatrix}+\frac{1}{6}\begin{bmatrix}2 & 1 & 0\\ 1 & 4 & 1\\ 0 & 1 & 2\end{bmatrix}\begin{bmatrix}\dot{u}_{i-1}\\ \dot{u}_i\\ \dot{u}_{i+1}\end{bmatrix}+\frac{\nu}{2l^{(e)}}\begin{bmatrix}-1 & 1 & 0\\ -1 & 0 & 1\\ 0 & -1 & 1\end{bmatrix}\begin{bmatrix}u_{i-1}\\ u_i\\ u_{i+1}\end{bmatrix}$$

$$+\frac{A}{6}\begin{bmatrix}2 & 1 & 0\\ 1 & 4 & 1\\ 0 & 1 & 2\end{bmatrix}\begin{bmatrix}u_{i-1}\\ u_i\\ u_{i+1}\end{bmatrix}=\frac{P}{2}\begin{bmatrix}1\\ 2\\ 1\end{bmatrix} \qquad (19)$$

Now put row corresponding to the node i to zero, from equation (19) the difference schemes with $l^{(e)} = h$ is:

$$\frac{1}{h^2}\left[-u_{i-1}+2u_i-u_{i+1}\right]+\frac{1}{6}\left[\dot{u}_{i-1}+4\dot{u}_i+\dot{u}_{i+1}\right]+\frac{\nu}{2h}\left[-u_{i-1}+u_{i+1}\right]+\frac{A}{6}\left[u_{i-1}+4u_i+u_{i+1}\right]=P \quad (20)$$

Applying the trapezoidal rule, following system of equations in Crank – Nicholson method are obtained:

$$A_1u_{i-1}^{n+1}+A_2u_i^{n+1}+A_3u_{i+1}^{n+1}=A_4u_{i-1}^{n}+A_5u_i^{n}+A_6u_{i+1}^{n}+12Pk \qquad (21)$$

Now from equations (12), (13) and (14), following equations are obtained:

$$B_1w_{i-1}^{n+1}+B_2w_i^{n+1}+B_3w_{i+1}^{n+1}=B_4w_{i-1}^{n}+B_5w_i^{n}+B_6w_{i+1}^{n}+12kAmu_i' \qquad (22)$$

$$G_1\theta_{i-1}^{n+1}+G_2\theta_i^{n+1}+G_3\theta_{i+1}^{n+1}=G_4\theta_{i-1}^{n}+G_5\theta_i^{n}+G_6\theta_{i+1}^{n}+12k(\mathrm{Pr})Ec\left(\frac{\partial u_i'}{\partial y}\right)^2 \qquad (23)$$

$$J_1C_{i-1}^{n+1}+J_2C_i^{n+1}+J_3C_{i+1}^{n+1}=J_4C_{i-1}^{n}+J_5C_i^{n}+J_6C_{i+1}^{n} \qquad (24)$$

Where $A_1 = 2 + Ak - 3vrh - 6r,\ A_2 = 4Ak + 12r + 8,\ A_3 = 2 + Ak + 3vrh - 6r$

$A_4 = 2 - Ak + 3vrh + 6r,\ A_5 = 8 - 4Ak - 12r,\ A_6 = 2 - Ak - 3vrh + 6r$

$B_1 = 2 + Ak - 3vrh - 6r,\ B_2 = 4Ak + 12r + 8,\ B_3 = 2 + Ak + 3vrh - 6r$

$B_4 = 2 - Ak + 3vrh + 6r,\ B_5 = 8 - 4Ah - 12r,\ B_6 = 2 - Ak - 3vrh + 6r$

$G_1 = 2(\mathrm{Pr}) - 3v(\mathrm{Pr})rh - 6r + Q(\mathrm{Pr})k,\ G_2 = 8(\mathrm{Pr}) + 12r + 4Q(\mathrm{Pr})k,$

$G_3 = 2(\mathrm{Pr}) + 3v(\mathrm{Pr})rh - 6r + Q(\mathrm{Pr})k,\ G_4 = 2(\mathrm{Pr}) + 3v(\mathrm{Pr})rh + 6rh - Q(\mathrm{Pr})k,$

$G_5 = 8(\mathrm{Pr}) - 12r - 4Q(\mathrm{Pr})k,\ G_6 = 2(\mathrm{Pr}) - 3v(\mathrm{Pr})rh + 6r - Q(\mathrm{Pr})k,$

$J_1 = 2(Sc) - 3v(Sc)rh - 6r,\ J_2 = 8(Sc) + 12r,\ J_3 = 2(Sc) + 3v(Sc)rh - 6r,$

$J_4 = 2(Sc) + 3v(Sc)rh + 6r,\ J_5 = 8(Sc) - 12r,\ J_6 = 2(Sc) - 3v(Sc)rh + 6r,$

$P = (Gr)\theta_i^j + (Gc)C_i^j - Amw_i^j$

Here $r = \dfrac{k}{h^2}$ and h, k are mesh sizes along y – direction and t – direction respectively. Index i refers to space and j refers to the time. In the equations (21), (22), (23) and (24) taking $i = 1(1)n$ and using boundary conditions (15), then the following system of equations are obtained:

$$A_i X_i = B_i \quad i = 1(1)4 \tag{25}$$

Where A_i's are matrices of order n and X_i, B_i's are column matrices having n – components. The solutions of above system of equations are obtained by using Thomas algorithm for primary velocity, secondary velocity, temperature and concentration. Also, numerical solutions for these equations are obtained by C – programme. In order to prove the convergence and stability of Galerkin finite element method, the same C – programme was run with smaller values of h and k and no significant change was observed in the values of u, w, θ and C. Hence the Galerkin finite element method is stable and convergent.

Knowing the velocity field the skin-friction at the wall along x' – axis in the dimensionless form is given by $\tau_1 = \left(\dfrac{\partial u}{\partial y}\right)_{y=0}$

Knowing the velocity field the skin–friction at the wall along z' – axis in the dimensionless form is given by $\tau_2 = \left(\frac{\partial w}{\partial y}\right)_{y=0}$

5.4 DISCUSSION OF THE RESULTS

The problem of Hall Effect on MHD flow and mass transfer of an electrically conducting incompressible fluid along an infinite vertical porous plate with viscous dissipation and heat absorption has been studied and solved by using Galerkin finite element method. The effects of material parameters such as Grashof number (Gr), Modified Grashof number (Gc) Prandtl number (Pr), Schmidt number (Sc), Hartmann number (M), Hall parameter (m), Eckert number (Ec), Heat absorption parameter (Q) and Transpiration cooling parameter (λ) separately in order to clearly observe their respective effects on the primary velocity, secondary velocity, temperature and concentration profiles of the flow. And also numerical values of skin friction coefficients (τ_1 & τ_2) have been discussed in table 1. We discussed the effects of material parameters on primary velocity profiles from figures (1) to (9), secondary velocity profiles from figures (10) to (18), temperature profiles from figures (19) to (22) and concentration profiles from the figures (23) and (24). During the course of numerical calculations of the primary velocity (u), secondary velocity (w), temperature (θ) and concentration (C) the values of the Prandtl number are chosen for Mercury (Pr = 0.025), Air at $25^{\circ}C$ and one atmospheric pressure (Pr = 0.71) and Water (Pr = 7.00). To focusout attention on numerical values of the results obtained in the study, the values of Sc are chosen for the gases representing diffusing chemical species of most common interest in air namely Hydrogen (Sc = 0.22), Helium (Sc = 0.30), Water–vapour (Sc = 0.60), Oxygen (Sc = 0.66) and Ammonia (Sc = 0.78). For the physical significance, the numerical discussions in the problem and at t = 1.0, stable values for primary velocity, secondary velocity, temperature and concentration fields are obtained. To examine the effect of parameters related to the problem on the velocity field and skin–friction numerical computations are carried out at Pr = 0.71. To find out the solution of this problem, we have placed an infinite vertical plate in a finite length in the flow. Hence, we solve the entire problem in a finite boundary. However, in the graphs, the y values vary from 0 to 4, and the

velocity, temperature, and concentration tend to zero as y tends to 4. This is true for any value of y. Thus, we have considered finite length.

The temperature and the species concentration are coupled to the velocity via Grashof number (Gr) and Modified Grashof number (Gc) as seen in equation (11). For various values of Grashof number and Modified Grashof number, the velocity profiles u are plotted in figures (1) and (2). The Grashof number (Gr) signifies the relative effect of the thermal buoyancy force to the viscous hydrodynamic force in the boundary layer. As expected, it is observed that there is a rise in the velocity due to the enhancement of thermal buoyancy force. Also, as Gr increases, the peak values of the velocity increases rapidly near the porous plate and then decays smoothly to the free stream velocity. The Modified Grashof number (Gc) defines the ratio of the species buoyancy force to the viscous hydrodynamic force. As expected, the fluid velocity increases and the peak value is more distinctive due to increase in the species buoyancy force. The velocity distribution attains a distinctive maximum value in the vicinity of the plate and then decreases properly to approach the free stream value. It is noticed that the velocity increases with increasing values of Modified Grashof number(Gc). The nature of primary velocity profiles in presence of foreign species such as Hydrogen ($Sc = 0.22$), Oxygen ($Sc = 0.60$) and Ammonia ($Sc = 0.78$) are shown in figure (3). The flow field suffers a decrease in primary velocity at all points in presence of heavier diffusing species.

The influence of the viscous dissipation parameter i.e., the Eckert number (Ec) on the velocity and temperature are shown in figures (4) and (20) respectively. The Eckert number (Ec) expresses the relationship between the kinetic energy in the flow and the enthalpy. It embodies the conversion of kinetic energy into internal energy by work done against the viscous fluid stresses. Greater viscous dissipative heat causes a rise in the temperature as well as the velocity. This behavior is evident from figures (4) and (20). Figure (5) depicts the effect of Prandtl number on primary velocity profiles in presence of foreign species such as Mercury ($Pr = 0.025$), Air ($Pr = 0.71$) and Water ($Pr = 7.00$) are shown in figure (5). We observe that from figure (5), the primary velocity decreases with increasing of Prandtl number (Pr). The effect of the Hartmann number (M) is shown in figure (6). It is observed that, the primary velocity of the fluid decreases with the

increasing of the magnetic field number values. The decrease in the primary velocity as the Hartmann number (M) increases is because the presence of a magnetic field in an electrically conducting fluid introduces a force called the Lorentz force, which acts against the flow, if the magnetic field is applied in the normal direction, as in the present study. This resistive force slows down the fluid velocity component as shown in figure (6).

Figure (7) depicts the primary velocity profiles as the Hall parameter m increases. We see that u increases as m increases. It can also be observed that u profiles approach their classical values when Hall parameter m becomes large ($m > 5$). Figures (8) and (21) illustrate the influence of Heat absorption parameter (Q) on the velocity and temperature at $t = 1.0$ respectively. Physically speaking, the presence of heat absorption (thermal sink) effects has the tendency to reduce the fluid temperature. This causes the thermal buoyancy effects to decrease resulting in a net reduction in the fluid velocity. These behaviors are clearly obvious from figures (8) and (21) in which both the velocity and temperature distributions decrease as (Q) increases. It is also observed that the both the hydrodynamic (velocity) and the thermal (temperature) boundary layers decrease as the heat absorption effects increase. From figure (9) shows that the primary velocity profiles against y for several values of the transpiration cooling parameter (λ) keeping other parameters of the flow field are constant. The transpiration cooling parameter is found to retard the primary velocity of the flow field at all points. The reduction in primary velocity at any point of the flow field is faster as the transpiration cooling parameter becomes larger. One interesting inference of this finding is greater transpiration cooling leads to a faster reduction in the primary velocity of the flow field.

In figure (16), we see that w profiles increase for $m < 1$ and decrease for $m > 1$. In figures (10) and (11), we see the influence of the both heat and mass transfer on secondary velocity of the flow. It can be seen that as both the heat and mass transfer increases, this velocity component increases as well. In figures (10) and (11), the effects of the heat and mass transfer on the velocity are displayed. It is apparent from the figures that, the increasing values of heat and mass transfer enhance the secondary velocity. The effect of Eckert number (Ec) on the secondary velocity flow field is presented in the figure (13). Here, the secondary velocity profiles are drawn against y for three different

values of Ec. The Eckert number is found to accelerate the secondary velocity of the flow field at all points.

In figure (15) we have the influence of the Hartmann number (M) on the secondary velocity. It can be seen that as the values of this parameter increases, the secondary velocity increases. The nature of secondary velocity profiles in presence of foreign species such as H_2 ($Sc = 0.22$), O_2 ($Sc = 0.60$) and NH_3 ($Sc = 0.78$) are shown in figure (12). The flow field suffers a decrease in secondary velocity at all points in presence of heavier diffusing species. Figure (14) depicts the effect of Prandtl number on secondary velocity profiles in presence of foreign species such as Mercury (Pr = 0.025), Air (Pr = 0.71) and Water (Pr = 7.00) are shown in figure (14). We observe that from figure (14) the velocity is decreasing with increasing of Prandtl number (Pr). The effect of Heat absorption parameter (Q) on the secondary velocity is as shown in the figure (17). From this figure the secondary velocity decreases with increasing values of Q .Figure (18) shows that the secondary velocity profiles against y for several values of the transpiration cooling parameter (λ). As the transpiration cooling parameter is to retard the secondary velocity.

In figure (19) we depict the effect of Prandtl number (Pr) on the temperature field. It is observed that an increase in the Prandtl number leads to decrease in the temperature field. Also, temperature field falls more rapidly for water in comparison to air and the temperature curve is exactly linear for mercury, which is more sensible towards change in temperature. From this observation it is conclude that mercury is most effective for maintaining temperature differences and can be used efficiently in the laboratory. Air can replace mercury, the effectiveness of maintaining temperature changes are much less than mercury. However, air can be better and cheap replacement for industrial purpose. This is because, either increase of kinematic viscosity or decrease of thermal conductivity leads to increase in the value of Prandtl number (Pr). Hence temperature decreases with increasing of Prandtl number (Pr). From figure (22) depicts the temperature profiles against y for various values of transpiration cooling parameter (λ) keeping other parameters are constant. Transpiration cooling parameter is found to decrease the temperature of the flow field at all points.

The effects of Transpiration cooling parameter (λ) and Schmidt number (Sc) on the concentration field are presented in figures (23) and (24). Figure (24) shows the concentration field due to variation in Schmidt number (Sc) for the gasses Hydrogen, Helium, Water – vapour, Oxygen and Ammonia. It is observed that concentration field is steadily for Hydrogen and falls rapidly for Oxygen and Ammonia in comparison to Water – vapour. Thus Hydrogen can be used for maintaining effective concentration field and Water – vapour can be used for maintaining normal concentration field. Figure (23) shows the plot of concentration distribution against y for different values of transpiration cooling parameter (λ) and fixed $Sc = 0.22$. A comparative study of the curves of the above figure shows that the concentration distribution of the flow field decreases faster as the transpiration cooling parameter (λ) becomes larger. Thus greater transpiration cooling leads to a faster decrease in concentration of the flow field.

Table (1) shows the variation of different values Gr, Gc, Sc, Pr, M, m, Ec, Q and λ. From this table it is concluded that the magnitude of shearing stress τ_1 and τ_2 increase as the value of Gr, Gc, m, Ec increase and this behavior is found just reverse with the increase of Pr, Sc, M, Q, λ. In order to ascertain the accuracy of the numerical results, the present skin – friction (τ_1) results are compared with the previous skin–friction (τ_1^*) results of Sriramulu *et al.* [23] in table 2. They are found to be in an excellent agreement.

Table 1: Variation of shearing stress τ_1 and τ_2 for different values of Gr, Gc, Sc, Pr, M, m, Ec, Q and λ

Gr	Gc	Pr	Sc	M	m	Ec	Q	λ	τ_1	τ_2
1.0	1.0	0.71	0.22	2.0	0.5	0.001	1.0	0.5	1.1507	0.2336
2.0	1.0	0.71	0.22	2.0	0.5	0.001	1.0	0.5	1.6979	0.3404
1.0	2.0	0.71	0.22	2.0	0.5	0.001	1.0	0.5	1.7544	0.3604
1.0	1.0	7.00	0.22	2.0	0.5	0.001	1.0	0.5	0.7697	0.1404
1.0	1.0	0.71	0.60	2.0	0.5	0.001	1.0	0.5	1.1070	0.2180
1.0	1.0	0.71	0.22	4.0	0.5	0.001	1.0	0.5	0.8314	0.1908
1.0	1.0	0.71	0.22	2.0	1.0	0.001	1.0	0.5	1.2552	0.4211
1.0	1.0	0.71	0.22	2.0	0.5	0.100	1.0	0.5	1.1537	0.2345
1.0	1.0	0.71	0.22	2.0	0.5	0.001	2.0	0.5	0.9824	0.1208
1.0	1.0	0.71	0.22	2.0	0.5	0.001	1.0	1.0	1.1482	0.2275

Table 2: Comparison of present Skin – friction results (τ_1) with the Skin – friction results (τ_1^*) obtained by Sriramulu *et al.* [23] for different values of Gr, Gc, Sc, Pr, M, m and λ

Gr	Gc	Pr	Sc	M	m	λ	τ_1	τ_1^*
1.0	1.0	0.71	0.22	2.0	0.5	0.5	1.1472	1.1469
2.0	1.0	0.71	0.22	2.0	0.5	0.5	1.4361	1.4353
1.0	2.0	0.71	0.22	2.0	0.5	0.5	1.6958	1.6941
1.0	1.0	7.00	0.22	2.0	0.5	0.5	0.6381	0.6365
1.0	1.0	0.71	0.60	2.0	0.5	0.5	1.0736	1.0725
1.0	1.0	0.71	0.22	4.0	0.5	0.5	0.7694	0.7685
1.0	1.0	0.71	0.22	2.0	1.0	0.5	1.2419	1.2410
1.0	1.0	0.71	0.22	2.0	0.5	0.5	1.1503	1.1501
1.0	1.0	0.71	0.22	2.0	0.5	1.0	1.1403	1.1395

OBSERVATIONS:

The Effects of primary velocity, secondary velocity, temperature and concentration for different parameters like Gr, Gc, Pr, Sc, M, m, λ, Q and Ec are studied. The study concludes the following results.

1. It is observed that both the primary (u) and secondary (w) velocities of the fluid increases with the increasing of parameters Gr, Gc, m, Ec and decreases with the increasing of parameters Pr, M, Q, Sc and λ.
2. The fluid temperature increases with the increasing of Ec and decreases with the increasing of Pr, Q and λ.
3. The Concentration of the fluid decreases with the increasing of λ and Sc.
4. From table (1) it is concluded that the magnitude of shearing stress τ_1 and τ_2 increases as the increasing values of Gr, Gc, m, Ec and this behavior is found just reverse with the increasing of Pr, Sc, M, Q and λ.

5.5 REFERENCES

[1] Abdul Maleque, Kh. and Abdur Sattar, Md., The Effects of Variable properties and Hall current on steady MHD laminar convective fluid flow due to a porous rotating disk. *Int. Journal of Heat and Mass Transfer*. 48, 4460 – 4466 (2005).

[2] Ajay Kumar Singh, MHD Free – convection and Mass Transfer Flow with Hall Current Viscous Dissipation, Joule Heating and Thermal Diffusion, *Indian Journal of Pure and Applied Physics*, 41, 24 – 35 (2003).

[3] Alam, M.M and Sattar, M.A., Unsteady free convection and mass transfer flow in a rotating system with Hall currents, viscous dissipation and Joul heating., Journal of Energy heat and mass transfer, 22, 31 – 39 (2000).

[4] Anand Rao, J. and Srinivasa Raju, R., Applied Magnetic Field on Transient Free Convective Flow of an Incompressible Viscous Dissipative Fluid in a Vertical Channel, *Journal of Energy, Heat and Mass Transfer*, 33, 313 – 332 (2010).

[5] Anand Rao, J. and Srinivasa Raju, R., Hall Effect on an unsteady MHD flow and heat transfer along a porous flat plate with mass transfer and viscous dissipation, *Journal of Energy, Heat and Mass Transfer*, 32, 265 – 277 (2011).

[6] Anjali Devi, S. P., Shailendhra, K., and Hemamalini, P. T., Pulsated convective MHD flow with Hall current, heat source and viscous dissipation along a vertical porous plate, *Int. J. of App. Math. and Computation*, 3(2), 141–150 (2011).

[7] Atul Kumar Singh, Ajay Kumar Singh and N. P. Singh, N. P., Hydromagnetic Free convection and Mass transfer flow with Joule heating, thermal diffusion, Heat source and Hall current, *Bulletin of the Institute of mathematics academia sinica*, 33(3), 291 – 310 (2005).

[8] Chamkha A.J., Unsteady MHD Convective Heat and Mass Transfer Past a Semi-Infinite Vertical Permeable Moving Plate with Heat Absorption, *Int. J. Eng. Sci.*, 42, 217 – 230 (2004).

[9] Chaudhary, R. C., Jain, P., Hall Effect on MHD mixed convection flow of a Viscoelastic fluid past an infinite vertical porous plate with mass transfer and radiation, *Ukr. J. Phys.*, 52(10), (2007).

[10] Chowdhary R. C. and Kumar Jha. A., Heat and mass transfer in elasticoviscous fluid past an impulsively started infinite vertical plate with Hall effect, *Latin America Applied Research*, 38, 17 – 26 (2008).

[11] Cookey C. I., Ogulu A., and Omubo-Pepple V. B., Influence of Viscous Dissipation and Radiation on Unsteady MHD Free-convection Flow Past an Infinit Heated Vertical Plate in a Porous Medium with Time Dependent Suction, *Int. J. Heat Mass Transfer.*, 46, 2305 – 2311 (2003).

[12] Emmanuel Osalusi, Jonathan Side, Robert Harris, Barry Johnston, On the Effectiveness of Viscous Dissipation and Joule Heating on Steady MHD and Slip Flow of a Bingham fluid over a porous rotating disk in the presence of Hall and ion-slip Currents, *Romanian Reports in Physics*, 61(1), 71 – 93 (2009).

[13] Hossain, M. A., and Rashid, R. I. M. A., Hall effects on Hydro magnetic Free Convection Flow along a Porous Flat Plate with Mass Transfer, *Journal of the Physical Society of Japan*, 56, 97 – 104 (1987).

[14] Lai, F. C., Coupled Heat and Mass Transfer by Mixed Convection from a Vertical Plate in a Saturated Porous Medium, *International Journal of Heat and Mass Transfer*, 18, 93 – 106 (1991).

[15] Maleque, K. A., Sattar, M. A., The effects of variable properties and hall current on steady MHD laminar convective fluid flow due to a porous rotating disk, *International Journal of Heat and Mass Transfer*, 48, 4963 – 4972 (2005).

[16] Palumbo, L. J., Platzeck, A. M., MHD stationary symmetric flows with Hall effect, *Journal of Plasma Physics*, 72, 457- 467 (2006).

[17] Rajashekhar, M. N., Anand Rao, J., and Shanker, B., Numerical Solutions of Hall Effects on Heat and Mass Transfer Flow through Porous Medium, *Journal of Energy Heat and Mass Transfer*, 21, 1 – 7 (1999).

[18] Singh, N. P., Mass Transfer effects on the Flow Past a vertical Porous Plate, *Proceedings of Math Soc.*, 12, 109 – 114 (1996).

[19] Singh, N. P., and Kumar, R., An Integral Treatment for Combined Heat and Mass Transfer by Natural Convention in a Porous Medium, *Acta Ciencia India*, 21, 451 – 463 (1995).

[20] Singh, N. P., Singh, A. K., and Kumar, R., Free Convection Heat and Mass Transfer along a Vertical Surface in a Porous Medium, *Indian Journal of Theoretical Physics*, 44, 255 – 264 (1996).

[21] Soundalgekar, V. M., Ray, S. N., and Dass, V. N., Coupled Heat and Mass transfer by Natural Convention from Vertical Surfaces in Porous Medium,

Proceedings of Math Soc., 11, 95 – 98 (1995).

[22] Srihari, K., Kishan, N., and Anand Rao, J., Hall Effect on MHD Flow and Heat Transfer along a Porous Flat Plate with Mass Transfer and Source/Sink, *Journal of Energy, Heat and Mass Transfer*, 30, 361 – 376 (2008).

[23] Sriramulu, A., Kishan, N., and Anand Rao, J., Effect of Hall Current on MHD Flow and Heat Transfer along a Porous Flat Plate with Mass Transfer, *J. Inst. Eng.* 87, 24 – 34 (2007).

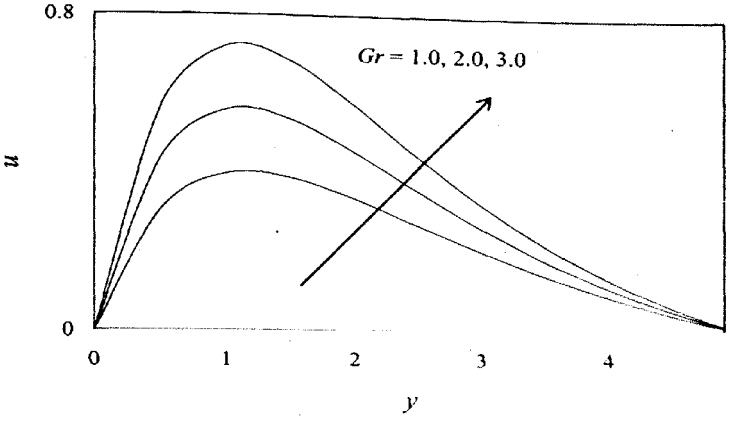

Figure 1. Effect of Grashof number Gr on primary velocity profiles u

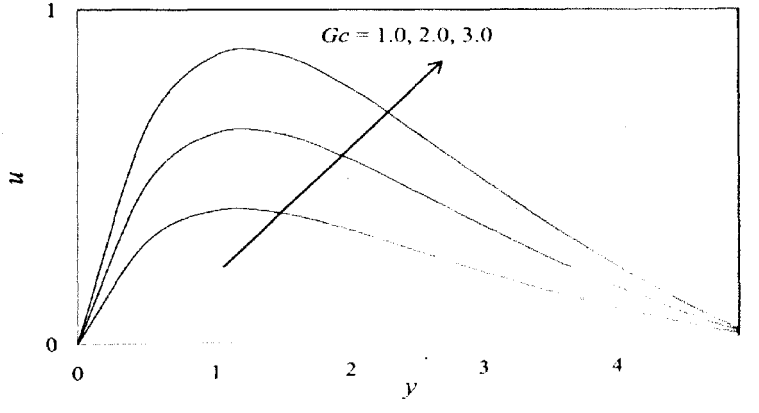

Figure 2. Effect of Modified Grashof number Gc on primary velocity profiles u

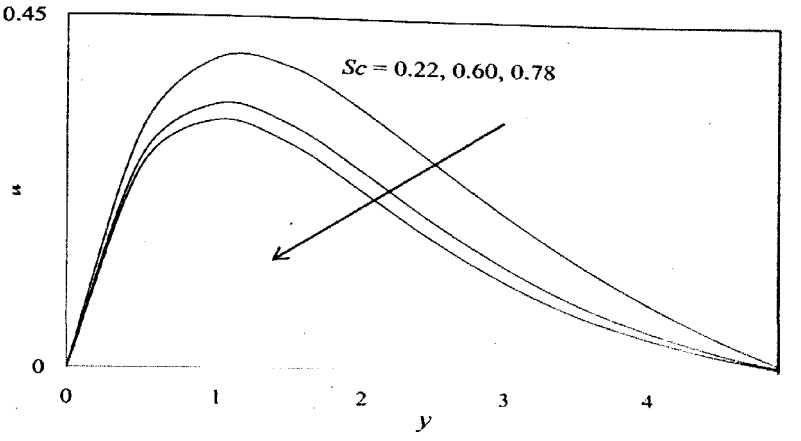

Figure 3. Effect of Schmidt number Sc on primary velocity profiles u

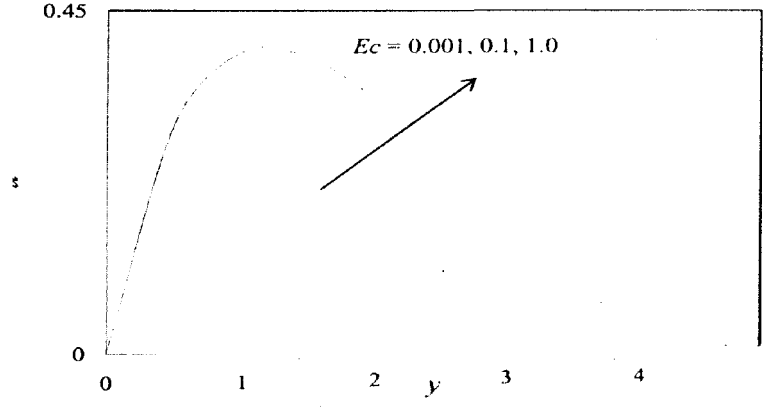

Figure 4. Effect of Eckert number Ec on primary velocity profiles u

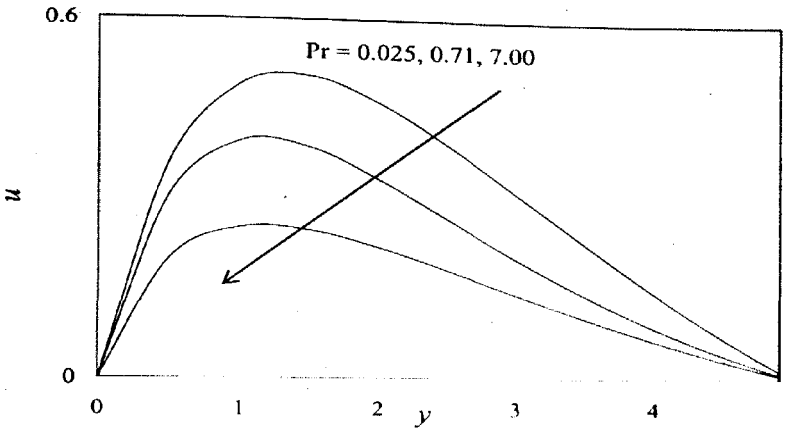

Figure 5. Effect of Prandtl number Pr on primary velocity profiles u

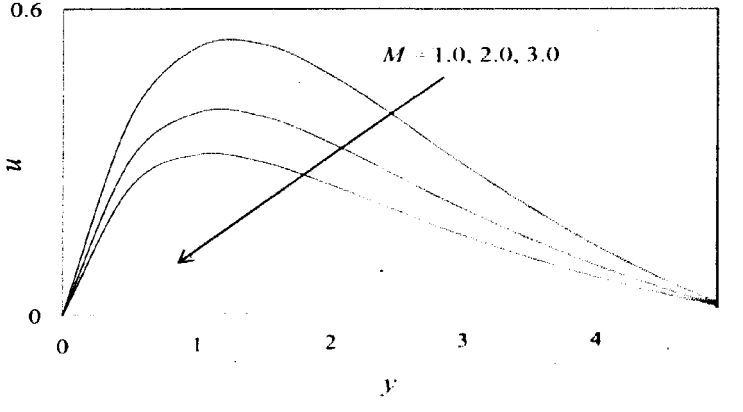

Figure 6. Effect of Hartmann number M on primary velocity profiles u

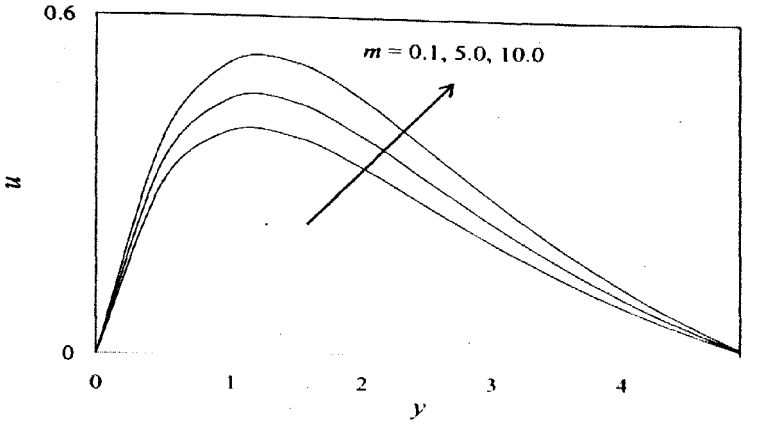

Figure 7. Effect of Hall parameter m on primary velocity profiles u

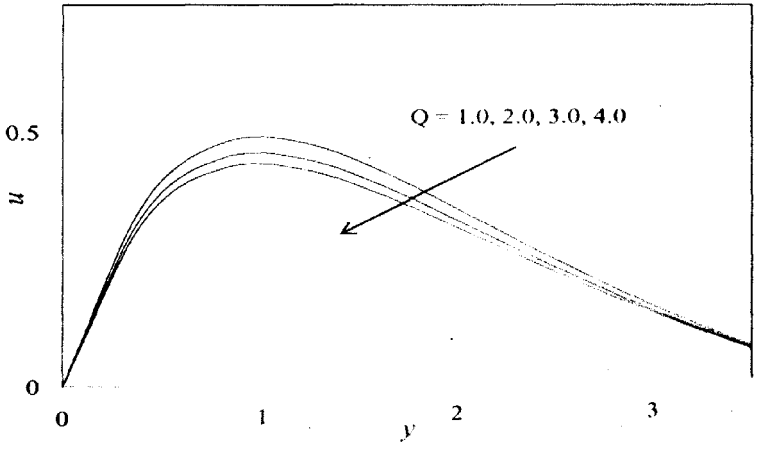

Figure 8. Effect of Heat absorption 'Q' on primary velocity profiles 'u'

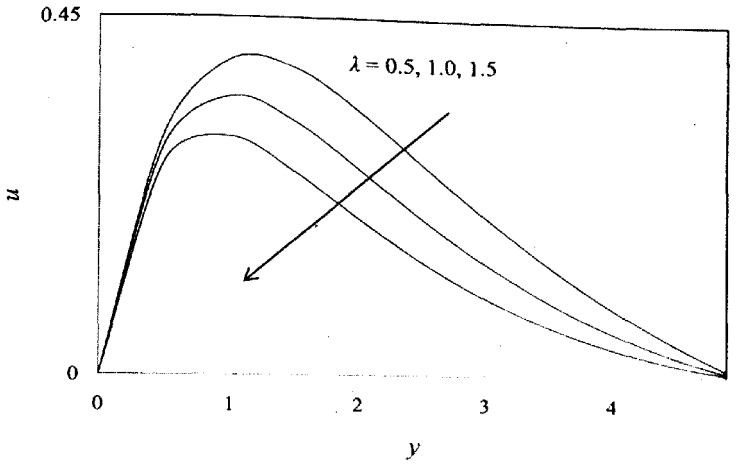

Figure 9. Effect of Transpiration cooling parameter λ on primary velocity profiles u

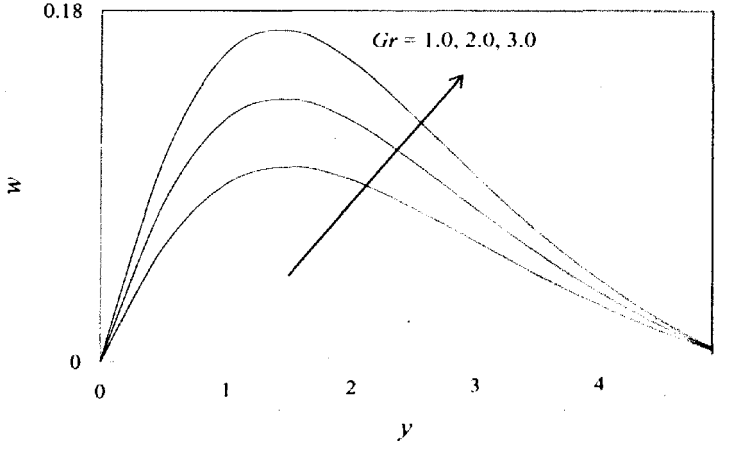

Figure 10. Effect of Grashof number Gr on secondary velocity profiles w

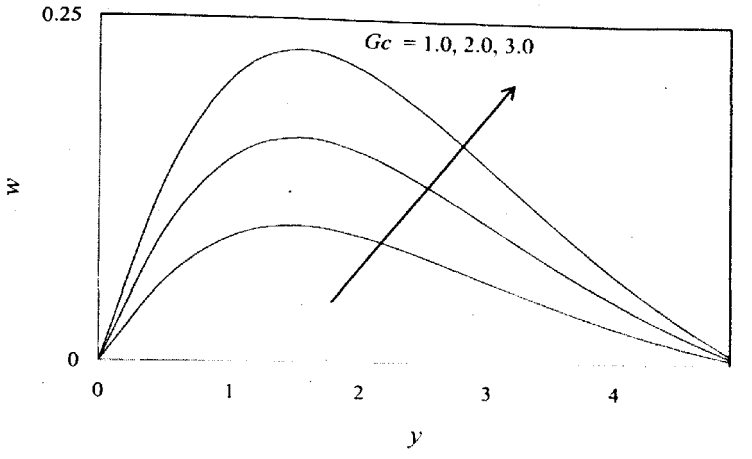

Figure 11. Effect of Modified Grashof number Gc on secondary velocity profiles w

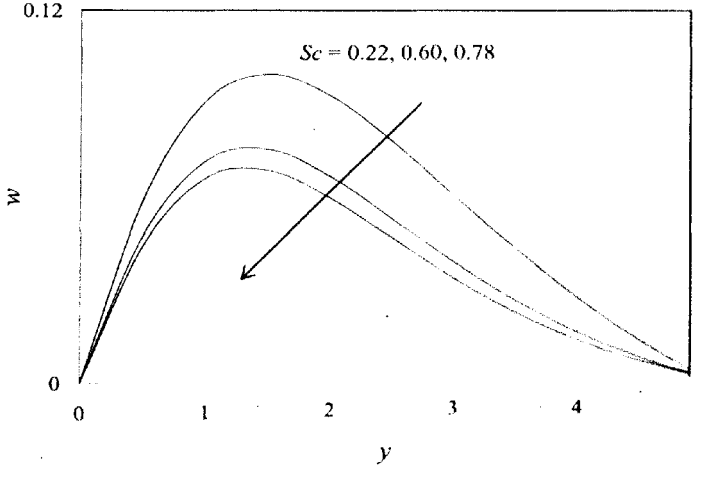

Figure 12. Effect of Schmidt number Sc on secondary velocity profiles w

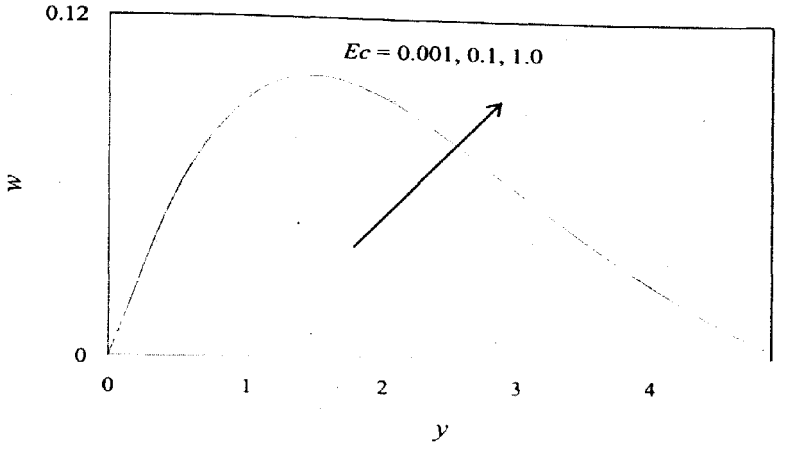

Figure 13. Effect of Eckert number Ec on secondary velocity profiles w

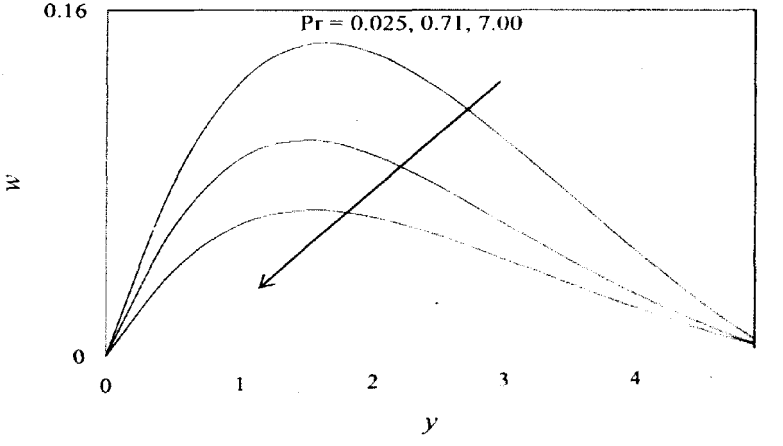

Figure 14. Effect of Prandtl number Pr on secondary velocity profiles w

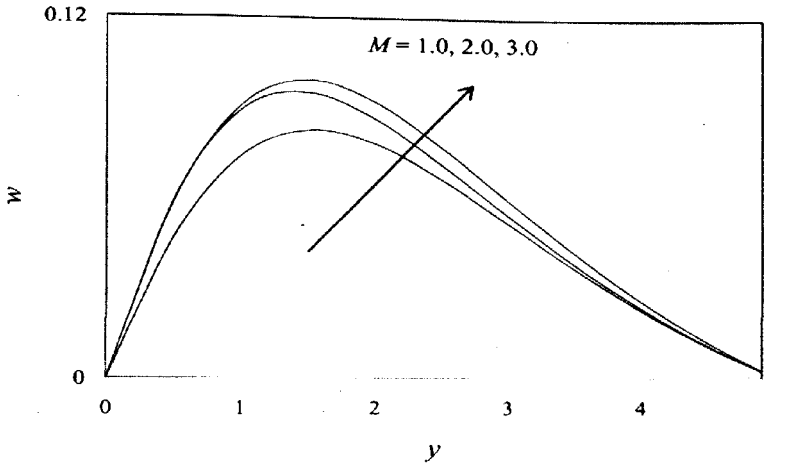

Figure 15. Effect of Hartmann number M on secondary velocity profiles w

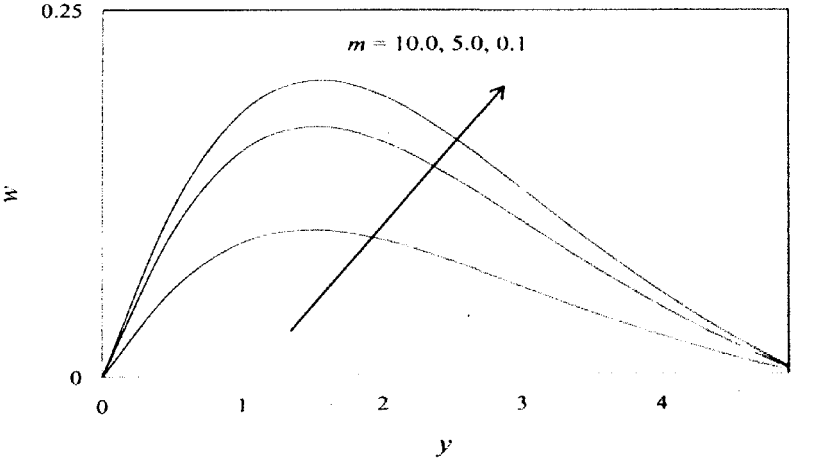

Figure 16. Effect of Hall parameter m on secondary velocity profiles w

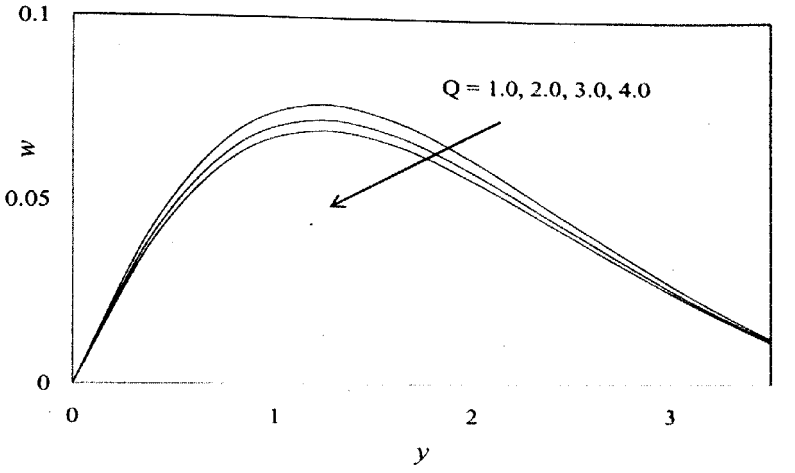

Figure 17. Effect of Heat absorption 'Q' on secondary velocity profiles 'w'

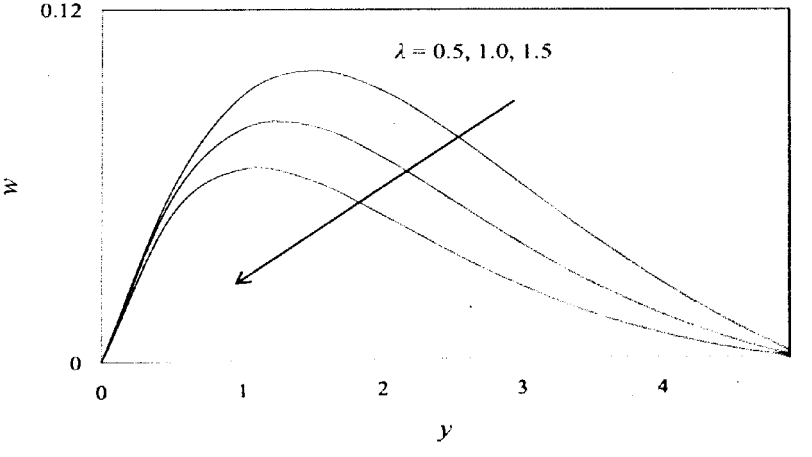

Figure 18. Effect of λ on secondary velocity profiles w

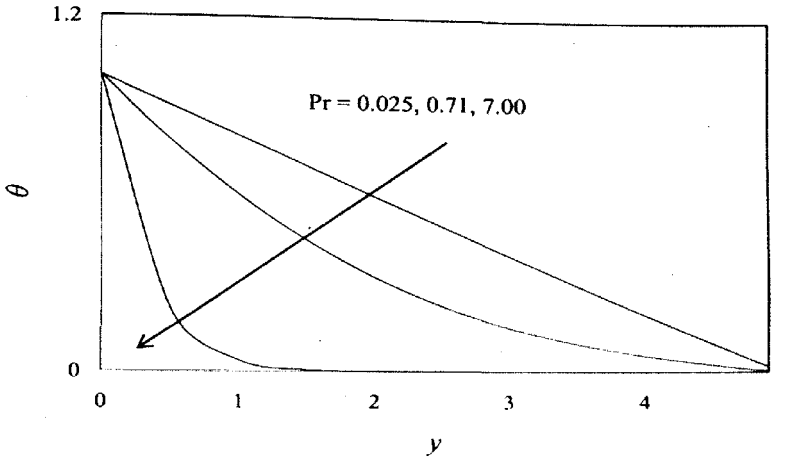

Figure 19. Effect of Prandtl number Pr on temperature profiles θ

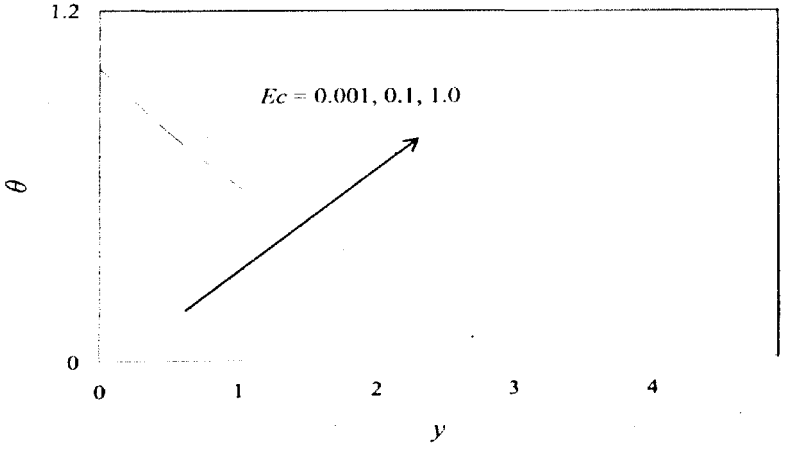

Figure 20. Effect of Eckert number Ec on temperature profiles θ

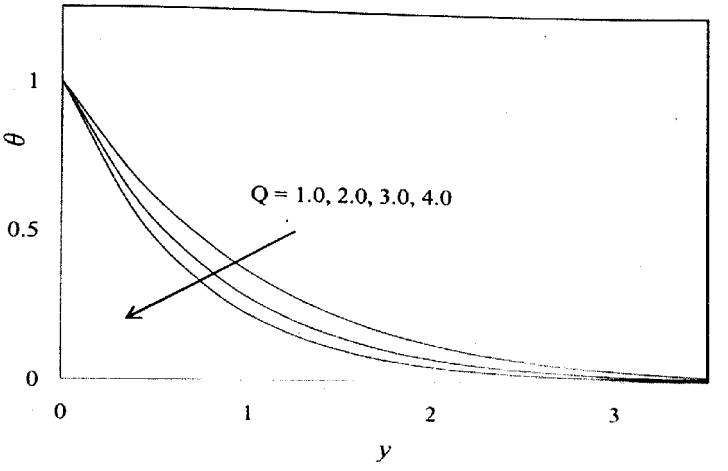

Figure 21. Effect of Heat absorption 'Q' on temperature profiles 'θ'

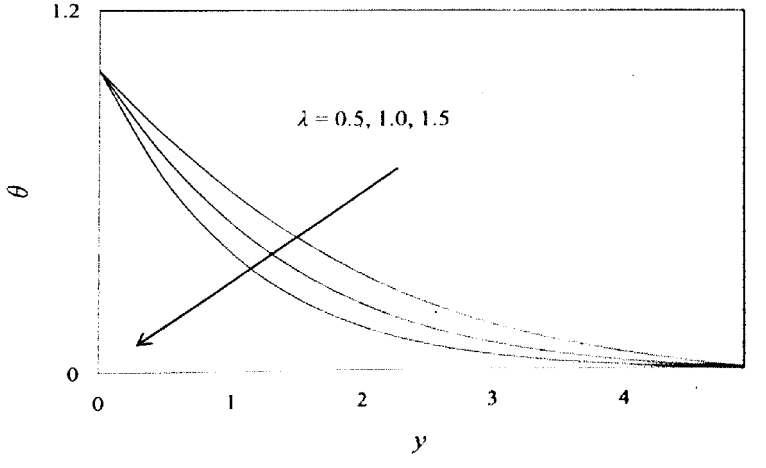

Figure 22. Effect of Transpiration cooling parameter λ on temperature profiles θ

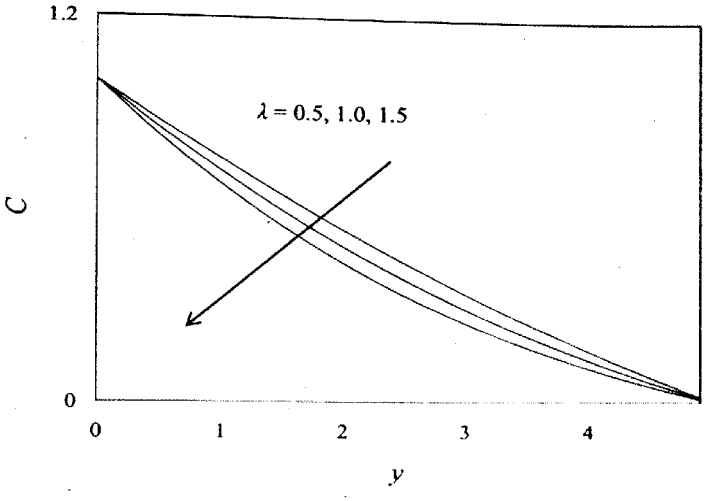

Figure 23. Effect of Transpiration cooling parameter λ on concentration profiles C

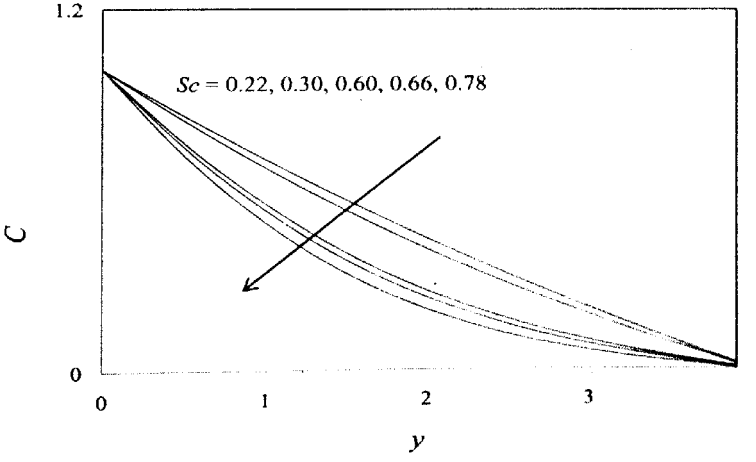

Figure 24. Effect of Schmidt number Sc on concentration profiles C